

# Recurrent Convolutional Fusion for RGB-D Object Recognition

Mohammad Reza Loghmani<sup>1</sup>

loghmani@acin.tuwien.ac.at

Mirco Planamente<sup>2</sup>

mirco.pl.93@gmail.com

Barbara Caputo<sup>3</sup>

Barbara.Caputo@iit.it

Markus Vincze<sup>1</sup>

vincze@acin.tuwien.ac.at

<sup>1</sup> Vision for Robotics, ACIN

TU Wien,

Vienna, Austria

<sup>2</sup> VANDAL laboratory,

Sapienza University of Rome,

Rome, Italy

<sup>3</sup> VANDAL laboratory,

Italian Institute of Technology,

Milan, Italy

---

## Abstract

Providing machines with the ability to recognize objects like humans has always been one of the primary goals of machine vision. The introduction of RGB-D cameras has paved the way for a significant leap forward in this direction thanks to the rich information provided by these sensors. However, the machine vision community still lacks an effective method to synergically use the RGB and depth data to improve object recognition. In order to take a step in this direction, we introduce a novel end-to-end architecture for RGB-D object recognition called recurrent convolutional fusion (RCFusion). Our method generates compact and highly discriminative multi-modal features by combining complementary RGB and depth information representing different levels of abstraction. Extensive experiments on two popular datasets, RGB-D Object Dataset and JHUIT-50, show that RCFusion significantly outperforms state-of-the-art approaches in both the object categorization and instance recognition tasks.

## 1 Introduction

Human-built environments are, ultimately, collections of objects. Every daily activity, such as cleaning or cooking, requires to understand and operate a set of objects to accomplish a task. Digital systems that aim at assisting the user in his own environment need to possess the ability to recognize objects. In fact, object recognition is the foundation for higher-level tasks that rely on an accurate description of the visual scene.

Despite the interesting results achieved for object recognition by operating on standard RGB images, there are inherent limitations due to the loss of data caused by projecting the 3-dimensional world into a 2-dimensional image plane. The use of RGB-D (Kinect-style) cameras potentially alleviates these shortcomings by using range imaging technologies to provide information about the camera-scene distance as a depth image. These sensors quickly became ubiquitous due to their affordable price and the rich visual information they provide. In fact, while the RGB image contains color, texture and appearance information,

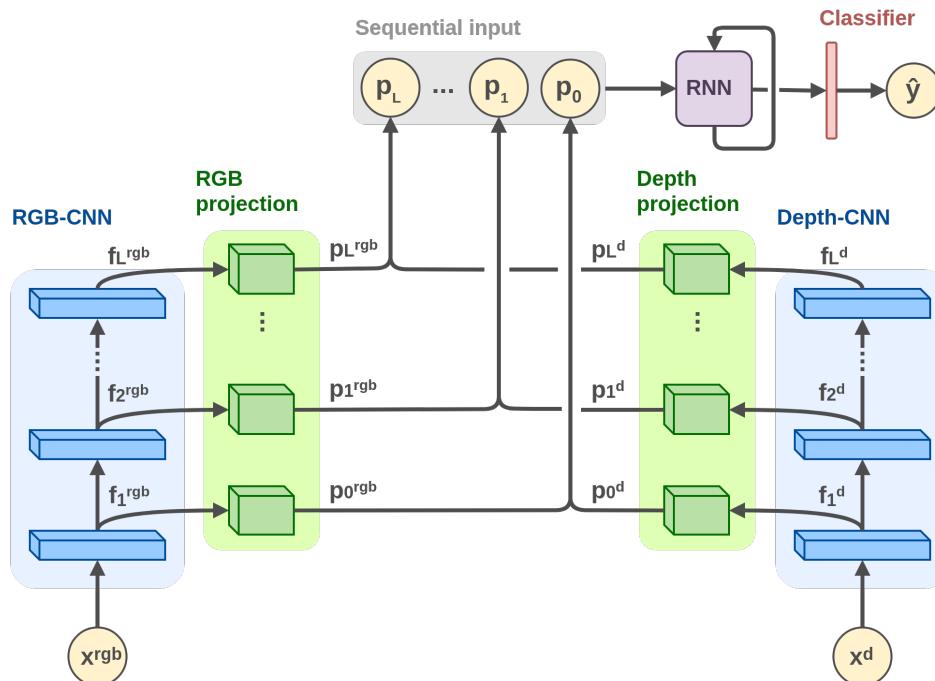


Figure 1: Architecture of recurrent convolutional fusion.

the depth image contains additional geometric information and is more invariant with respect to lighting and color variations.

After the pivotal work of Krizhevsky *et al.* [22], deep convolutional neural networks (CNNs) quickly became the dominant tool in computer vision, establishing new state-of-the-art results for a large variety of tasks, such as human pose estimation [10], semantic segmentation [9] and image super-resolution [24]. Research in RGB-D object recognition followed the same trend, with numerous algorithms (e.g. [4, 11, 12, 17, 26, 34]) exploiting features learned from CNNs instead of the traditional hand-crafted features. The common pipeline involves two CNN streams, operating on RGB and depth images respectively, as feature extractors. However, the lack of a large-scale dataset of depth images to train the depth CNN forced the machine vision community to find practical workarounds. A significant amount of effort has been dedicated to develop methods that colorize the depth images in order to exploit CNNs pre-trained on RGB images. However, the actual strategies to extract and combine the features from the two modalities have been neglected. In fact, several methods simply rely on a trivial concatenation of the features extracted from a specific layer of the two CNNs that are then fed to a classifier. We argue that this strategy is sub-optimal because (a) it is based on the assumption that the selected layer always represents the best abstraction level to combine RGB and depth information and (b) no explicit mechanism ensures that the diverse characteristics of the two modalities are properly exploited.

In this paper, we propose a novel end-to-end architecture for RGB-D object recognition called recurrent convolutional fusion (RCFusion). Our method extracts features from multiple hidden layers of the CNNs for RGB and depth, respectively, and combines them through a recurrent neural network (RNN), as shown in figure 1. In addition, we formulate a loss function to promote orthogonality between corresponding RGB and depth features, assisting the two streams in learning complementary information. With extensive experiments, we show that the combination of complementary features representing different levels of abstraction, produces a highly discriminative description of the RGB-D data. We evaluate our method on standard object recognition benchmarks, RGB-D Object Dataset [23] and JHUIT-50 [25],

and we compare the results with the best performing methods in the literature. The experimental results show that our method outperforms the existing approaches and establishes new state-of-the-art results for both datasets. An implementation of the method, relying on tensorflow [3], will be released upon acceptance of the paper.

The remainder of the paper is organized as follows: the next section positions our approach compared to related work, section 3 introduces the proposed method, section 4 reveals the implementation details, section 5 presents the experimental results and section 6 draws the conclusions.

## 2 Related Work

The diffusion of RGB-D cameras fueled an increasing effort in designing visual algorithms able to exploit the additional depth information provided by these sensors. Classical approaches for RGB-D object recognition (e.g. [6, 23]) used a combination of different hand-crafted feature descriptors, such as SIFT, textons, and depth edges, on the two modalities (RGB and depth) to perform object matching. More recently, several methods have exploited shallow learning techniques to generate features from RGB-D data in an unsupervised learning framework [5, 7, 32]. These methods rely on algorithms such as hierarchical matching pursuit [7], k-means clustering [27] and RNNs [21] to progressively build higher level features in an unsupervised fashion.

Since the ground-breaking work of Krizhevsky *et al.* [22], data-hungry deep CNNs have been the to-go solution for feature extraction [16, 30]. While large-scale datasets of RGB images, such as ImageNet [15], allowed the generation of powerful CNN-based models for RGB feature extraction, the lack of a depth counterpart posed the problem of how to extract features from depth images. An effective and convenient strategy to circumvent the problem is to colorize the depth images to exploit CNNs pre-trained on RGB data. Several hand-crafted colorization approaches have been proposed to map the raw depth value of each pixel [17] or derived physical quantities, such as position and orientation [19] or local surface normals [8], to colors. Carlucci *et al.* [12] proposed instead a learning-based approach to colorize the depth images by training a colorization network. Other methods used alternatives to RGB-trained CNNs for extracting features from depth data. Li *et al.* [26] generated the depth features using a modified version of HONV [33] encoded with Fisher Vector [29]. Carlucci *et al.* [11] generated artificial depth data using 3D CAD models to train a CNN that extracts features directly from raw depth images.

The aforementioned methods focused on effectively extracting features from the depth data and used trivial strategies to combine the two modalities for the final prediction. Very few works prioritized this latter aspect. Wang *et al.* [34] alternatively maximized the discriminative characteristics of each modality and minimized the inter-modality distance in feature space. Wang *et al.* [35] obtained the multi-modal feature by using a custom layer to separate the individual and correlated information of the extracted RGB and depth features. Both methods combined the two modalities by processing features extracted from one layer of the CNNs and relied on cumbersome multi-stage optimization processes.

The focus of this paper is on the synthesis of multi-modal features from RGB-D data rather than the depth processing. In fact, for the depth processing part, we adopt the well known colorization method based on surface normals, since it has been proved to be effective and robust across tasks [4, 8, 35]. Differently from existing works, our method does not rely on features extracted from one specific layer of a CNN, but combines features extracted from

multiple layers to generate the final multi-modal representation. In addition, our model can be trained in all together, without the need of optimizing in multiple stages.

### 3 Recurrent Convolutional Fusion

Our multi-modal deep neural network for RGB-D object recognition is illustrated in figure 1. The network’s architecture has three main stages:

1. *multi-level feature extraction*: two streams of convolutional networks, with the same architecture, are used to process RGB and depth data (RGB-CNN and Depth-CNN), respectively, and extract features at different levels of the networks;
2. *feature projection and concatenation*: features extracted from each level of the RGB- and Depth-CNN are individually transformed through projection blocks and then concatenated to create the corresponding RGB-D feature;
3. *recurrent multi-modal fusion*: RGB-D features extracted from different levels are sequentially fed to an RNN that produces a descriptive and compact multi-modal feature.

The output of the recurrent network is then used by a softmax classifier to infer the object label. The network can be trained end-to-end using standard backpropagation algorithms based on stochastic gradient descent. The loss function to minimize is composed of two terms: a standard classification loss and an orthogonality loss, that encourages the RGB and depth features to represent complementary information. In the following, we describe in greater detail each of the aforesaid characteristics of RCFusion.

#### 3.1 Multi-level feature extraction

CNNs process the input with sets of filters learned from a large amount of data. These filters represent progressively higher levels of abstraction, going from the input to the output: edges, textures, patterns, parts, and objects [28, 36]. Methods for RGB-D object recognition commonly combine the output of one of the last layers of the RGB- and Depth-CNN to obtain the final multi-modal feature. This strategy is based on the strong assumption that the chosen layer represents the appropriate level of abstraction to combine the two modalities. We argue that it is possible to remove this assumption by combining RGB and depth information at multiple layers across the CNNs and use them all to generate a highly discriminative RGB-D feature. Let us denote with  $x^{rgb} \in \mathcal{X}^{rgb}$  the RGB input images, with  $x^d \in \mathcal{X}^d$  the depth input images and  $y \in \mathcal{Y}$  the labels, where  $\mathcal{X}^{rgb}$ ,  $\mathcal{X}^d$  and  $\mathcal{Y}$  are the RGB/depth input and label space. We further denote with  $f_i^{rgb}$  and  $f_i^d$  the output of layer  $i$  of RGB-CNN and Depth-CNN, respectively, with  $i = 1, \dots, L$  and  $L$  the total number of layers of each CNN. As previously mentioned, the RGB- and Depth-CNN are assumed to have the same architecture.

#### 3.2 Feature projection and concatenation

One of the main challenges in combining features obtained from different hidden layers is the lack of a one-to-one correspondence between elements of the different feature vectors. More formally,  $f_i^*$  and  $f_j^*$ , with  $i \neq j$  and  $*$  indicating any of the superscripts  $rgb$  or  $d$ , have (in general) different dimensions and thus belong to distinct feature spaces,  $\mathcal{F}_i$  and  $\mathcal{F}_j$ . In order to make features coming from different levels of abstraction comparable, we project them into a common space  $\bar{\mathcal{F}}$ :

$$p_i^* = G_i^*(f_i^*) \quad \text{s.t.} \quad p_i^* \in \bar{\mathcal{F}} \quad \forall i. \quad (1)$$

The projection function  $G(\cdot)$  performs a set of non-linear operations defined by pooling and convolutional layers (see section 4 for the specific implementation). The projected RGB and depth features of each layer  $i$  are then concatenated to form  $p_i = [p_i^{rgb}; p_i^d]$ .

### 3.3 Recurrent multi-modal fusion

In order to create a compact multi-modal representation, the set  $\{p_1, \dots, p_L\}$  is sequentially fed to an RNN. Recurrent models align the positions of the elements in the sequence to steps in computation time and generate a sequence of hidden states  $h_i$  as a function of the previous hidden state  $h_{i-1}$  and the current input  $p_i$ . The choice of a recurrent network for this operation is twofold: (a) the hidden state of the network acts as a memory unit and embeds a summary of the most relevant information from the different levels of abstraction, and (b) the number of parameters of the network is independent of  $L$ , while for a more straightforward choice, such as a fully connected layer, it grows linearly with  $L$ . The output of the RNN is used by the softmax classifier for the final prediction  $\hat{y}$ .

### 3.4 Loss

RCFusion can be trained end-to-end using standard backpropagation. The loss function

$$\mathcal{L} = \mathcal{L}_{\text{cls}} + \mathcal{L}_{\perp} \quad (2)$$

is minimized during training with respect to the parameters of the network. The first term of equation 2 is the classification loss  $\mathcal{L}_{\text{cls}}$  that trains the model to predict the output labels we are ultimately interested in. It is defined as a cross-entropy loss

$$\mathcal{L}_{\text{cls}} = - \sum_{j=1}^S y_j \log \hat{y}_j, \quad (3)$$

where  $S$  is the number of available training samples. We propose to regularize the training by adding an orthogonality loss  $\mathcal{L}_{\perp}$  that imposes a soft orthogonality constraint between the projected RGB and depth features. Let  $P_i^{rgb}$  and  $P_i^d$  be matrices whose rows are the projected features  $p_i^{rgb}$  and  $p_i^d$ . The orthogonality loss  $\mathcal{L}_{\perp}$  is defined as

$$\mathcal{L}_{\perp} = \sum_{i=1}^L \lambda_i \left\| P_i^{rgbT} P_i^d \right\|_F^2, \quad (4)$$

where  $\lambda_i$  denotes the weight of the regularization for layer  $i$ ,  $\|\cdot\|_F^2$  is the squared Frobenius norm, and the superscript  $T$  denotes the transpose operator. The purpose of  $\mathcal{L}_{\perp}$  is to minimize the overlapping information carried by the projected features to properly exploit the unique characteristics of the two modalities.

## 4 Implementation details

This section aims at fully disclosing the implementational choices of the version of RC-Fusion used in this paper to enable the repeatability of the experiments. In particular, we provide here the specific instantiation of the different parts composing the network: RGB-/Depth-CNN, projection blocks and RNN. Nonetheless, it is important to keep in mind that

the concepts described in section 3 are agnostic to the specific implementation and can be adapted to the task at hand.

**RGB-/Depth-CNN:** With computational and memory efficiency in mind, we chose a CNN architecture with a limited number of parameters. Since residual networks have become a standard choice, we deployed ResNet-18, the most compact representation proposed by He *et al.* [20]. ResNet-18 has 18 convolutional layers organized in five residual blocks, for a total of approximately 40,000 parameters. An implementation of the network pre-trained on ImageNet is available in [1].

**Projection blocks:** The projection blocks transform a volumetric input into a vector of dimensions  $(1 \times p_d)$  through two convolutional layers and a global max pooling layer. We designed the block in such a way that the first convolutional layer focuses on exploiting the spatial dimensions, width and height, of the input with  $p_d$  filters of size  $(7 \times 7)$ , while the second convolutional layer exploits its depth with  $p_d$  filters of size  $(1 \times 1)$ . Finally, the global max pooling computes the maximum of each depth slice. This instantiation of the projection blocks has provided the best performances among those that we tried.

**RNN:** In a trade-off between network capacity and limited number of parameters, we used a popular recurrent network called gated recurrent unit (GRU) [13]. This network is considered to be a variation of long-short term memory (LSTM) [21] and its effectiveness in dealing with long input sequences has been repeatedly shown [14]. Despite performing comparably, GRU requires 25% fewer parameters than LSTM. In our experiments, we process the sequence of projected vectors with a single GRU layer with a number of memory neurons  $m_n$ . An implementation of GRU can be found in all the most popular deep learning libraries, including tensorflow.

## 5 Experiments

In the following, we evaluate RCFusion on RGB-D Object Dataset and JHUIT-50. After revealing the protocol used to set up the experiments, we discuss the strategies and the hyper-parameters used for training the network. Finally, we showcase the performance of our model and highlight its strengths and weaknesses.

### 5.1 Setup

We evaluate our algorithm on two popular RGB-D datasets representing objects: RGB-D Object Dataset and JHUIT-50. RGB-D Object Dataset contains 41,877 RGB-D images capturing 300 objects from 51 categories, spanning from fruit and vegetables to tools and containers. Since its introduction, this dataset has become the silver thread connecting the existing methods for RGB-D object recognition. We use this dataset to assess the performance of RCFusion in the object categorization task. For the evaluation, we follow the standard experimental protocol defined in [6], where ten training/test split are defined in such a way that one object instance per class is left out of the training set. The reported results are the average accuracy over the different splits. JHUIT-50 contains 14,698 RGB-D images capturing 50 common workshop tools, such as clamps and screw drivers. Since this dataset presents few objects, but very similar to each others, it can be used to assess the performance of RCFusion in the instance recognition task. For the evaluation, we follow the standard experimental protocol defined in [25], where training data are collected from fixed viewing angles between the camera and the object while the test data are collected by freely moving

Ablation study						
Loss	res1-5	res2-5	res3-5	res4-5	res5 only	output
w/ $\mathcal{L}_\perp$	94.0±1.1	94.3±1.0	94.4±1.4	94.0±1.1	-	-
w/o $\mathcal{L}_\perp$	93.9±1.3	94.2±1.7	94.2±1.1	94.0±1.4	94.0±1.7	93.9±1.0

Table 1: Accuracy (%) of different configurations of our method: *resA – B* indicates that the features are extracted from residual block *A* until *B* of ResNet-18 and *output* indicates the output of the final residual block; w/(o)  $\mathcal{L}_\perp$  indicates that the orthogonality loss is included (or not) in the optimization process.

the camera around the object. As stated in section 2, we colorize the depth images of both datasets with surface normal encoding and adopt the pre-processing procedure used in [4].

## 5.2 Training

We trained our model using RMSprop optimizer [2] with batch size 64, learning rate 0.001, momentum 0.9, weight decay 0.0002 and max norm 4. The weight  $\lambda_i$ , indicating the influence of the orthogonality loss for layer *i*, is set to 0.0001 for lower layers and decreases moving toward the output of the network. The architecture specific parameters have been fixed through a grid search to projection depth  $pd = 512$  and memory neurons  $mn = 50$ . The weights of the two ResNet-18 used as the RGB- and Depth-CNN are initialized with values obtained by pre-training the networks on ImageNet. The rest of the network is initialized with Xavier initialization method [18] in a multi-start fashion, where the network is initialized multiple times and, after one epoch, only the most promising model continues the training. For JHUIT-50, we compensate for the small training set of about 7,000 images with simple data augmentation techniques: scaling, horizontal and vertical flip, 90 degree rotation.

## 5.3 Results

We perform a series of experiments to demonstrate the capabilities of our method and analyze its behavior in different cases. First, we isolate the contribution on the two main components of RCFusion, multi-level feature extraction and orthogonality loss. Then, we provide some hints to understand the behavior of the method by analyzing its performance on specific object categories. Finally, we compare it with the existing methods in the literature. For sake of compactness, the ablation study and the analysis are performed on the RGB-D Object Dataset, while the benchmark includes also the results on JHUIT-50 to demonstrate the robustness of our method against changes in datasets and tasks.

**Ablation study:** To observe how the inclusion of features from multiple level of abstraction influences the performance of the network, we progressively consider features extracted from lower layers of ResNet-18. More precisely, we start from the output of the last residual block (output) and go backwards until the first residual block (res1). We repeat the same experiments by removing  $\mathcal{L}_\perp$  from the loss function. The results in table 1 show that the sole inclusion of lower level features can improve the accuracy of the network from 93.9% up to 94.2%. When including  $\mathcal{L}_\perp$  in the optimization process, the accuracy can further increase up to 94.4%. It is worth pointing out that the weight  $\lambda_i$  for layers higher than the fourth residual block is set to zero, thus motivating the missing values in table 1.

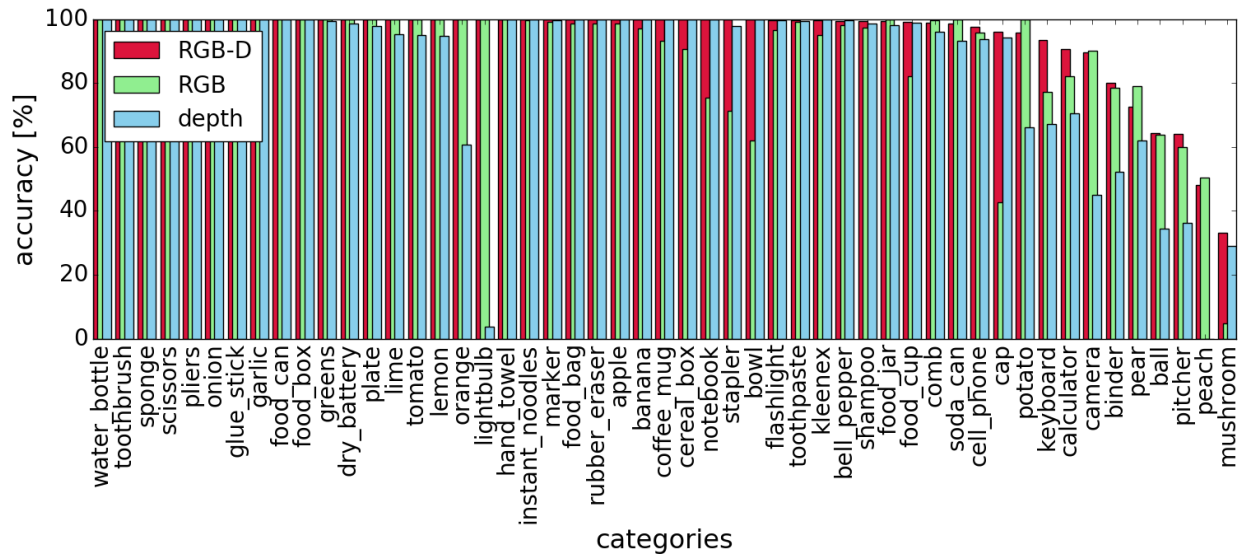


Figure 2: Per class accuracy (%) of RCFusion on RGB-D Object Dataset [23].

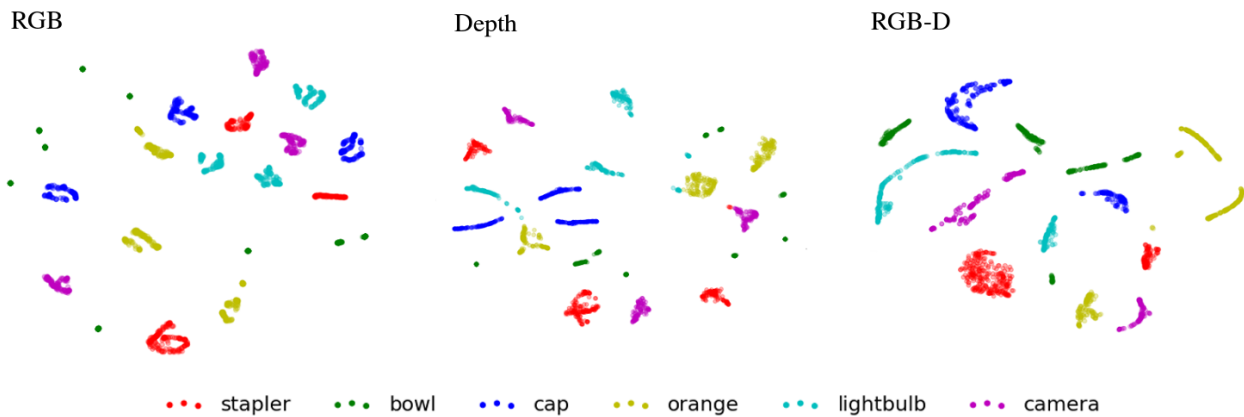


Figure 3: t-SNE visualization of the final features obtained for RGB, depth and RGB-D modalities.

**Analysis:** In order to gain a better insight on the performances of RCFusion, we consider the accuracy on the individual categories of RGB-D Object Dataset. Figure 2 shows that the multi-modal approach either matches or improves over the results on the single modalities for almost all categories. For categories like "lightbulb", "orange" or "bowl", where the accuracy on one modality is very low, RCFusion learns to rely on the other modality. This can be intuitively seen from the t-SNE visualization of the final features of the different modalities in figure 3, where the RGB-D features of each category appear in fewer, more compact clusters. An interesting insight on the functioning of the method is given by examining, for each category, which other categories generate the misclassification (confusion). When an object class is confused with the same classes in both RGB and depth modalities, like for "pear" and "potato", the RGB-D modality can perform slightly worse than the single modalities. This highlights a weakness of the method that will be the subject of future investigations. Instead, when an object class is confused with distinct classes in the individual modalities, like for "keyboard" and "calculator", the RGB-D modality can perform better.

**Benchmark:** We benchmark RCFusion on RGB-D Object Dataset and JHUIT-50 against other methods in the literature. Table 2 shows the results on RGB-D Object Dataset



RGB-D Object Dataset			
Method	RGB	Depth	RGB-D
LMMMDL [34]	74.6±2.9	75.5±2.7	86.9±2.6
FusionNet [17]	84.1±2.7	83.8±2.7	91.3±1.4
CNN w/ FV [26]	<b>90.8</b> ±1.6	81.8±2.4	<b>93.8</b> ±0.9
DepthNet [11]	88.4±1.8	83.8±2.0	92.2±1.3
CIMDL [35]	87.3±1.6	<b>84.2</b> ±1.7	92.4±1.8
FusionNet enhanced [4]	<b>89.5</b> ±1.9	<b>84.5</b> ±2.9	<b>93.5</b> ±1.1
DECO [12]	<b>89.5</b> ±1.6	84.0±2.3	<b>93.6</b> ±0.9
RCFusion – output	<b>89.6</b> ±2.2	<b>85.9</b> ±2.7	<b>93.9</b> ±1.0
RCFusion – res3-5	<b>89.6</b> ±2.2	<b>85.9</b> ±2.7	<b>94.4</b> ±1.4

Table 2: Accuracy (%) of several methods for object recognition on RGB-D Object Dataset [23]. Red: highest result; blue: other considerable results.

JHUIT-50			
Method	RGB	Depth	RGB-D
DepthNet [11]	88.0	55.0	90.3
FusionNet enhanced [4]	<b>94.7</b>	56.0	<b>95.3</b>
DECO [12]	<b>94.7</b>	<b>61.8</b>	<b>95.7</b>
RCFusion (ours)	<b>95.1</b>	<b>59.8</b>	<b>97.7</b>

Table 3: Accuracy (%) of several methods for object recognition on JHUIT-50 [25]. Red: highest result; blue: other considerable results.

for the object categorization task. For the individual modalities, ResNet-18 demonstrates to be a valid trade-off between limited number of parameters and high accuracy. In fact, our accuracy on the RGB modality is second only to [26], where they use a VGG network [31] that introduces considerably more parameters than ResNet-18. For the depth modality, ResNet-18 provides higher accuracy than all the competing methods. More importantly, in the multi-modal RGB-D classification, our method clearly outperforms all the competing approaches. It is worth noticing that, when we extract the features only from the output of the last residual layer (RCFusion – output), we perform comparably to the best existing methods. However, when including lower level features, our method gains a 0.6% over [26]. This highlights, once again, the importance of multi-level feature extraction and orthogonality loss as the main contributions of this paper. Table 3 shows the results on JHUIT-50 for the instance recognition task. For the individual modalities, ResNet-18 shows again a compelling performance. In the multi-modal RGB-D classification, our method clearly outperforms all the competing approaches with a margin of 2% on [12]. In summary, RCFusion establishes new state-of-the-art results on the two most popular datasets for RGB-D object recognition, demonstrating its robustness against changes in the dataset and the task.

## 6 Discussion and conclusion

In this paper, we have presented RCFusion: a multi-modal deep neural network for RGB-D object recognition. Our method uses two streams of convolutional networks to extract RGB and depth features from multiple levels of abstraction. These features are then concatenated and sequentially fed to an RNN to obtain a compact RGB-D feature that is used by a softmax

classifier for the final classification. An orthogonality loss is also adopted to encourage the two streams to learn complementary information. With thorough experiments on RGB-D Object Dataset and JHUIT-50, we show how each component of the method contributes to the final performance and allows RCFusion to outperform the existing methods in the literature. Due to their implementation-agnostic nature, the main concepts presented in this paper can be adapted to different tasks. In fact, the results obtained on object categorization encourage further research to extend this approach to higher level tasks, such as object detection and semantic segmentation.

## References

- [1] Resnet-18 caffemodel on imagenet. <https://github.com/HolmesShuan/ResNet-18-Caffemodel-on-ImageNet>. Accessed: 21-04-2018.
- [2] Overview of mini-batch gradient descent - lecture slides. [http://www.cs.toronto.edu/~tijmen/csc321/slides/lecture\\_slides\\_lec6.pdf](http://www.cs.toronto.edu/~tijmen/csc321/slides/lecture_slides_lec6.pdf). Accessed: 26-04-2018.
- [3] Tensorflow. <https://www.tensorflow.org/>. Accessed: 24-04-2018.
- [4] A. Aakerberg, K. Nasrollahi, and T. Heder. Improving a deep learning based rgb-d object recognition model by ensemble learning. In *IEEE International Conference on Image Processing Theory, Tools and Applications*, pages 1–6, 2017.
- [5] M. Blum, J. T. Springenberg, J. Wülfing, and M. Riedmiller. A learned feature descriptor for object recognition in rgb-d data. In *IEEE International Conference on Robotics and Automation (ICRA)*, pages 1298–1303, 2012.
- [6] L. Bo, X. Ren, and D. Fox. Depth kernel descriptors for object recognition. In *IEEE/RSJ International Conference on Intelligent Robots and Systems (IROS)*, pages 821–826, 2011.
- [7] L. Bo, X. Ren, and D. Fox. Hierarchical matching pursuit for image classification: Architecture and fast algorithms. In *Advances in Neural Information Processing Systems (NIPS)*, pages 2115–2123, 2011.
- [8] L. Bo, X. Ren D., and Fox. *Unsupervised Feature Learning for RGB-D Based Object Recognition*, pages 387–402. 2013.
- [9] Z. Cao, T. Simon, S. Wei, and Y. Sheikh. Mask r-cnn. In *IEEE International Conference on Computer Vision (ICCV)*, pages 2961–2969, 2017.
- [10] Z. Cao, T. Simon, S. Wei, and Y. Sheikh. Realtime multi-person 2d pose estimation using part affinity fields. In *IEEE Conference on Computer Vision and Pattern Recognition (CVPR)*, pages 7291–7299, 2017.
- [11] F. Carlucci, P. Russo, and B. Caputo. A deep representation for depth images from synthetic data. In *IEEE International Conference on Robotics and Automation (ICRA)*, pages 1362–1369, 2017.

- [12] F. M. Carlucci, P. Russo, and B. Caputo. (DE)<sup>2</sup>CO: Deep depth colorization. *IEEE Robotics and Automation Letter (RA-L)*, 3(3):2386–2396, 2018.
- [13] K. Cho, B. van Merriënboer, Ç. Gülçehre, D. Bahdanau, F. Bougares, H. Schwenk, and Y. Bengio. Learning phrase representations using rnn encoder–decoder for statistical machine translation. In *Conference on Empirical Methods in Natural Language Processing (EMNLP)*, pages 1724–1734, 2014.
- [14] J. Chung, Ç. Gülçehre, K. Cho, and Yoshua Bengio. Empirical evaluation of gated recurrent neural networks on sequence modeling. *CoRR*, abs/1412.3555, 2014.
- [15] J. Deng, W. Dong and R. Socher, L. Li, K. Li, and F. Li. Imagenet: A large-scale hierarchical image database. In *Proceedings of IEEE Conference on Computer Vision and Pattern Recognition (CVPR)*, pages 248–255, 2009.
- [16] J. Donahue, Y. Jia, O. Vinyals, J. Hoffman, N. Zhang, E. Tzeng, and T. Darrell. Decaf: A deep convolutional activation feature for generic visual recognition. In *International Conference on Machine Learning (ICML)*, volume 32, pages 647–655, 2014.
- [17] A. Eitel, T. Springenberg, L. Spinello M. Riedmiller, and W. Burgard. Multimodal deep learning for robust rgb-d object recognition. In *IEEE/RSJ International Conference on Intelligent Robots and Systems (IROS)*, pages 681–687, 2015.
- [18] X. Glorot and Y. Bengio. Understanding the difficulty of training deep feedforward neural networks. In *International Conference on Artificial Intelligence and Statistics (AISTATS)*, volume 9, pages 249–256, 2010.
- [19] S. Gupta, R. Girshick, P. Arbeláez, and J. Malik. Learning rich features from rgb-d images for object detection and segmentation. In *Computer Vision – ECCV 2014*, pages 345–360, 2014.
- [20] K. He, X. Zhang, S. Ren, and J. Sun. Deep residual learning for image recognition. In *Proceedings of IEEE Conference on Computer Vision and Pattern Recognition (CVPR)*, pages 770–778, 2016.
- [21] S. Hochreiter and J. Schmidhuber. Long short-term memory. *Neural Computation*, 9(8):1735–1780, 1997.
- [22] A. Krizhevsky, I. Sutskever, and G.E. Hinton. Imagenet classification with deep convolutional neural networks. In *Advances in Neural Information Processing Systems (NIPS)*, pages 1097–1105, 2012.
- [23] K. Lai, L. Bo, X. Ren, and D. Fox. A large-scale hierarchical multi-view rgb-d object dataset. In *IEEE International Conference on Robotics and Automation (ICRA)*, pages 1817–1824, 2011.
- [24] C. Ledig, L. Theis, F. Huszár, J. Caballero, A. Cunningham, A. Acosta, A. Aitken, A. Tejani, J. Totz, Z. Wang, and W. Shi. Photo-realistic single image super-resolution using a generative adversarial network. In *IEEE Conference on Computer Vision and Pattern Recognition (CVPR)*, pages 4681–4690, 2016.

- [25] C. Li, J. Bohren, E. Carlson, and G. D. Hager. Hierarchical semantic parsing for object pose estimation in densely cluttered scenes. In *IEEE International Conference on Robotics and Automation (ICRA)*, pages 5068–5075, 2016.
- [26] W. Li, Z. Cao, Y. Xiao, and Z. Fang. Hybrid rgb-d object recognition using convolutional neural network and fisher vector. In *Chinese Automation Congress (CAC)*, pages 506–511, 2015.
- [27] J. MacQueen. Some methods for classification and analysis of multivariate observations. In *Berkeley Symposium on Mathematical Statistics and Probability, Volume 1: Statistics*, pages 281–297. University of California Press, 1967.
- [28] C. Olah, A. Mordvintsev, and L. Schubert. Feature visualization. *Distill*, 2017. <https://distill.pub/2017/feature-visualization>.
- [29] F. Perronnin, J. Sánchez, and T. Mensink. Improving the fisher kernel for large-scale image classification. In *European Conference on Computer Vision (ECCV)*, pages 143–156, 2010.
- [30] A.S. Razavian, H. Azizpour, J. Sullivan, and S. Carlsson. Cnn features off-the-shelf: an astounding baseline for recognition. In *IEEE Conference on Computer Vision and Pattern Recognition (CVPR)*, pages 806–813, 2014.
- [31] K. Simonyan and A. Zisserman. Very deep convolutional networks for large-scale image recognition. *CoRR*, abs/1409.1556, 2014.
- [32] R. Socher, B. Huval, B. Bhat, C. D. Manning, and A. Y. Ng. Convolutional-recursive deep learning for 3d object classification. In *Advances in Neural Information Processing Systems (NIPS)*, pages 656–664, 2012.
- [33] S. Tang, X. Wang, X. Lv, T.X. Han, J. Keller, Z. He, M. Skubic, and S. Lao. Histogram of oriented normal vectors for object recognition with a depth sensor. In *Asian Conference on Computer Vision (ACCV)*, pages 525–538, 2013.
- [34] A. Wang, J. Lu, J. Cai, T. J. Cham, and G. Wang. Large-margin multi-modal deep learning for rgb-d object recognition. *IEEE Transactions on Multimedia*, 17(11):1887–1898, 2015.
- [35] Z. Wang, R. Lin, J. Lu, J. Feng, and J. Zhou. Correlated and individual multi-modal deep learning for RGB-D object recognition. *CoRR*, abs/1604.01655, 2016.
- [36] M.D. Zeiler and R. Fergus. Visualizing and understanding convolutional networks. In *Computer Vision – ECCV 2014: 13th European Conference, Proceedings, Part I*, pages 818–833, 2014.